

# Maximum possible energies of electrons accelerated in magnetospheres of rotating black holes

N. Nikuradze<sup>1</sup> and Z.N. Osmanov<sup>1,2</sup>

<sup>1</sup> School of Physics, Free University of Tbilisi, 0183, Tbilisi, Georgia  
e-mail: nniku21@freeuni.edu.ge

<sup>2</sup> E. Kharadze Georgian National Astrophysical Observatory, Abastumani 0301, Georgia e-mail: z.osmanov@freeuni.edu.ge

Received September 15, 1996; accepted March 16, 1997

## ABSTRACT

**Aims.** To evaluate the maximum attainable energies of electrons accelerated by means of the magneto-centrifugal mechanism. We examine how the range of maximum possible energies, as well as the primary limiting factors, vary with black hole mass. Additionally, we analyze the dependence of the maximum relativistic factor on an initial distance from the black hole.

**Methods.** To model the acceleration of electrons on rotating magnetic field lines we apply several constraining mechanisms: the inverse Compton scattering, curvature radiation and the breakdown of the bead-on-the-wire approximation.

**Results.** The maximal Lorentz factors for electron acceleration vary with the type of a black hole. For stellar-mass black holes, electrons can be accelerated up to the Lorentz factors  $2 \times 10^6 - 2 \times 10^8$  with only co-rotation constrain affecting the maximal relativistic factor; In intermediate-mass black holes, the Lorentz factors are in the interval  $2 \times 10^8 - 2 \times 10^{11}$ ; For the supermassive black holes the Lorentz factors range from  $2.5 \times 10^{10}$  to  $2 \times 10^{15}$ ; while the ultra-massive black hole located at the center of Abell 1201 can accelerate electrons up to  $1.1 \times 10^{13} - 6.6 \times 10^{16}$ . with both the co-rotation and curvature radiation determining the final Lorentz factor for the last three categories

**Key words.**

Use \titlerunning to supply a shorter title and/or \authorrunning to supply a shorter list of authors.

## 1. Introduction

Mainly, there are three types of black holes based on their mass: stellar-mass black holes with  $M_{BH} < 10^2 M_\odot$ , intermediate mass black holes (IMBH) with  $10^2 M_\odot < M_{BH} < 10^5 M_\odot$ , and supermassive black holes (SMBH) with  $M_{BH} > 10^5 M_\odot$ . Sometimes, another group of ultra-massive black holes is added, such as the one in the center of Abell 1201 with  $M_{BH} = 3.27 \times 10^{10} M_\odot$ , which was discovered via gravitational lensing (Nightingale et al. 2023). Although stellar-mass and supermassive black holes have been detected, the existence of intermediate-mass black holes (IMBHs) remains uncertain. There are potential locations where IMBHs could exist, such as one that might reside at the center of the globular cluster 47 Tucanae, as suggested by (Kiziltan et al. 2017). However, this has yet to be definitively confirmed. Proposing a new method of measuring the mass of a black hole would help us to unravel the mystery concerning IMBHs or verify the old data. Our method links the mass of a black hole to its ability to accelerate electrons with its magnetic field.

In cosmic ray astrophysics one of the major problems is to understand mechanisms, which provide high energies. The so-called Fermi acceleration (Fermi 1949) and its modifications (Bell 1978a,b; Catanese & Weekes 1999), although might explain particle acceleration to relativistic energies, but as it turned out, the mechanism is efficient if the particles are already pre-accelerated (Rieger & Mannheim 2000). The efficiency of the Blandford-Znajek process (Blandford & Znajek 1977), is significantly reduced by means of the screening effects.

The prevailing characteristic of black holes is their tendency to rotate, accompanied by the co-rotation of their magnetic field lines. Electrons, caught within the magnetic field, undergo a trajectory governed by the Lorentz force, resulting in a spiral path. The synchrotron emission rapidly diminishes the electron's perpendicular momentum, confining its motion primarily along the magnetic field lines. In particular, one can straightforwardly estimate that the synchrotron cooling time-scale,  $\tau_s \approx \gamma m_e c^2 / P_s$  ( $\gamma$  and  $m_e$  are the electron's relativistic factor and mass respectively,  $c$  denotes the speed of light,  $P_e \approx 2e^4 B^2 \gamma^2 / (3m_e^2 c^3)$  is the synchrotron emission power,  $e$  is the electron's charge and  $B$  denotes the magnetic induction) is of the order of  $10^{-2} s$ , which is smaller than the rotation period of a black hole,  $P \approx 2\pi(GM_{BH})/c^3 \approx 1230s$  where  $M_{BH} = 10^6 M_\odot$ . This means that the particles, soon after they accelerate, lose their perpendicular momentum, transit to the ground Landau state and proceed sliding along the field lines. The rotation of the magnetic field induces a centrifugal force on the electrons, leading to their acceleration. However, this acceleration is limited due to the counteracting effects of mechanisms such as inverse Compton scattering and curvature radiation, which cause the energy loss process. Consequently, electrons reach a maximum energy level determined by the equilibrium between acceleration and energy loss mechanisms. Furthermore, electrons may attain a critical energy threshold at which they break off the magnetic field line, setting an additional constraint on their maximal energy. Similar phenomenon has been studied in active galactic nuclei (AGN) by Osmanov et al. (2007). The authors investigated efficiency of centrifugal acceleration of electrons as possible mechanism for the generation of ultra - high energy  $\gamma$  -ray emission in TeV

blazars and studied the phenomenon for various inclination angles of magnetic field lines. Additionally, it has been shown that electrons can attain  $\gamma_{max} \approx 10^8$  with constraining factor of inverse Compton scattering. Moreover, the acceleration process has been studied by [Osmanov & Rieger \(2009\)](#) and reviewed by [Osmanov \(2021\)](#) for high energy  $\gamma$ -ray pulsars. This study focused on three constraining factors: inverse Compton scattering, curvature radiation and co-rotation. It has been shown that maximal Lorentz factor of  $10^7$  can be achieved. While the effectiveness of centrifugal acceleration as a mechanism in black holes has been previously explored, studies have not been focused on black hole mass and the initial radial coordinate as primary parameters. Our research addresses this gap by examining the acceleration mechanism across a broad spectrum of black hole masses. Particularly, we focus on intermediate-mass black holes (IMBHs) and the ultra-massive black hole (UMBH) at the center of Abell 1201. We assess the efficiency of this acceleration process within black hole magnetospheres with masses spanning  $1 - 10^9 M_{\odot}$  and for the black hole at the center of Abell 1201 with mass  $3.27 \times 10^{10} M_{\odot}$ . We consider magnetic field lines to be straight and Our study accounts for constraints from inverse Compton scattering, curvature radiation, and co-rotation effects. Additionally, We analyze how the relativistic factor and the main constraining factor depend on the distance from the BH.

## 2. Acceleration process

In this section we consider a black hole with mass  $M_{BH}$  which rotates at angular velocity  $\Omega \approx \frac{c^3}{40GM_{BH}}$  ( $a = 0.1$ ) ([Shapiro & Teukolsky 1983](#)). We consider electrons moving along the magnetic field line in the rotating plane. The motion of electrons along curved trajectories was thoroughly investigated by [Rogava et al. \(2003\)](#). While our study focuses on straight magnetic field lines in the horizontal plane, the work by [Rogava et al. \(2003\)](#) serves as a crucial foundational reference for our research. Electron's motion is described in polar coordinates where coordinate, velocity and acceleration can be written as:

$$\mathbf{r} = r \cdot \mathbf{e}_r \quad (1)$$

$$\mathbf{v} = \frac{d\mathbf{r}}{dt} = \dot{r} \cdot \mathbf{e}_r + r\dot{\theta} \cdot \mathbf{e}_\phi \quad (2)$$

$$\mathbf{a} = \frac{d\mathbf{v}}{dt} = (\ddot{r} - \Omega^2 r) \cdot \mathbf{e}_r + 2\dot{r}\dot{\theta} \cdot \mathbf{e}_\phi \quad (3)$$

$$\gamma = \frac{1}{\sqrt{1 - \frac{v^2}{c^2}}} = \frac{1}{\sqrt{1 - \frac{\dot{r}^2 + r^2\dot{\theta}^2}{c^2}}} \quad (4)$$

Force in the polar coordinates is derived from the derivative of electron's momentum

$$\mathbf{F} = \frac{d\mathbf{P}}{dt} = \frac{d(\gamma m_e \mathbf{v})}{dt} = m_e \left( \frac{\dot{r}^2(\ddot{r} + \Omega^2 r)}{c^2(1 - (\frac{v}{c})^2)^{\frac{3}{2}}} + \frac{\ddot{r} - \Omega^2 r}{(1 - (\frac{v}{c})^2)^{\frac{1}{2}}} \right) \cdot \mathbf{e}_r + F_\theta \cdot \mathbf{e}_\theta \quad (5)$$

Only force acting on the electron in the radial direction is gravitational force (Figure 1). Due to small spinning factor, the most of the acceleration process happens far from the BH, hence gravitational force is negligible. Therefore,  $F_r = 0$  (in a lab frame)

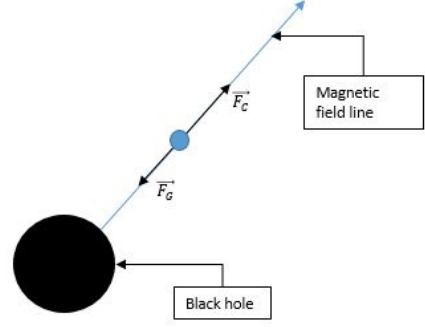
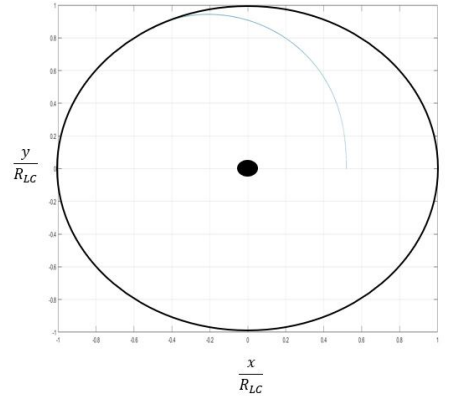
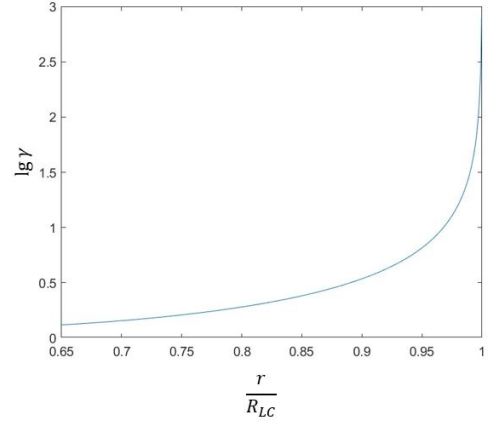


Fig. 1: Force diagram in the rotating frame



(a)



(b)

Fig. 2: (a) Electron trajectory (Blue curve), Black disk in the middle is the BH and outer black circle is the LC (b) The Lorentz factor dependence on the radial distance

gives rise to the final equation describing the acceleration process of the electron.

$$\ddot{r} = \Omega^2 r \frac{1 - \frac{\Omega^2 r^2}{c^2} - \frac{2\dot{r}^2}{c^2}}{1 - \frac{\Omega^2 r^2}{c^2}} \quad (6)$$

After solving equation (6), we can see two very interesting results that are depicted in Fig. 2 parts (a) and (b). First result is

that the electron doesn't go outside a certain zone called the light cylinder (LC - a hypothetical area where the linear velocity of rotation exactly equals the speed of light). Tangential velocity of the electron is less than the speed of light so  $\Omega r < c \Rightarrow r < \frac{c}{\Omega} \Rightarrow r_{max} = \frac{c}{\Omega} = \frac{40GM_{BH}}{c^2} \equiv R_{LC}$ . When the electron approaches the LC, its tangential velocity  $v_\theta \rightarrow c$ . Therefore, the radial velocity approaches zero. So if the electron is bounded to the straight magnetic field line, it can never leave the LC radius ( $R_{LC}$ ). From the Fig. 2 (b) we can see that the Lorentz factor of the electrons increases rapidly near the LC and it would have gone to infinity if no constraining factors occurred. A very interesting analytical result can be inferred from the equation of motion. It appears that dependence of Lorentz factor on radial distance is as follows:

$$\gamma = \gamma_0 \frac{1 - \frac{r_0^2}{R_{LC}^2}}{1 - \frac{r^2}{R_{LC}^2}} \quad (7)$$

where  $\gamma_0$  and  $r_0$  are initial Lorentz factor and radial distance respectively (Rieger 2011; Osmanov & Rieger 2016).

### 3. Constraining factors

In this section we consider different types of constraining factors.

#### 3.1. Co-Rotation Constraint

In the acceleration process, we have considered that the electron follows the magnetic field line. However, if the energy of the electron grows too large, it flies off the field line, and the acceleration process stops. Therefore, the electron reaches its maximum relativistic factor. Co-rotation constraint is satisfied if the magnetic field energy density,  $B^2/8\pi$ , exceeds the plasma energy density  $\gamma n_{GJ} M m_e c^2$ , where  $B$  denotes the magnetic field induction ( $B = 2\sqrt{\pi\rho v^2}$ , where  $\rho$  and  $v$  are calculated through the Bondi spherical accretion model (Bondi 1952) and results in the following expression of the magnetic field  $B \approx (\frac{\pi\rho_\infty}{2\sqrt{2}a_\infty})^{\frac{1}{2}} (\frac{GM_{BH}}{r})^{\frac{5}{4}}$  and equals to  $2.35 \cdot 10^3 G$  at  $r = R_{LC} = \frac{40GM}{c^2}$ ,  $\rho_\infty \approx 10^{-24} \frac{g}{cm^3}$ ,  $a_\infty \approx 10^6 \frac{cm}{s}$  where  $\rho_\infty$  and  $a_\infty$  are hydrogen density and sound speed very far from the BH respectively) and  $n_{GJ} = \Omega B / (2\pi e c)$  is the Goldreich–Julian number density of electrons (Goldreich & Julian 1969),  $e$  is the electron's charge, and  $M$  is the multiplicity factor of particles.

$$\frac{B^2}{8\pi} \geq \gamma n_{GJ} m_e c^2 \Rightarrow \gamma \leq \frac{Be}{4\Omega m_e c} \quad (8)$$

Since the electron has to rotate with the magnetic field line, it at least has tangential velocity which makes Lorentz factor to be greater than its minimum value.

$$\gamma = \left(1 - \frac{v^2}{c^2} - \frac{r^2 \Omega^2}{c^2}\right)^{\frac{1}{2}} \geq \left(1 - \frac{r^2 \Omega^2}{c^2}\right)^{\frac{1}{2}} \quad (9)$$

#### 3.2. Inverse Compton effect

The area inside the LC zone of the BH is filled with thermal photons radiated from an accretion disk. The electron collides with photons and loses energy. This effect is called Inverse Compton (IC) effect. In general, the IC scattering might occur in two extreme regimes, in the so-called Thomson regime for very low

energy particles and in the Klein–Nishina regime for very energetic electrons. In particular, the former takes place if the following condition is satisfied  $\gamma \epsilon_{ph} / (m_e c^2) \ll 1$  and in the latter case  $\gamma \epsilon_{ph} / (m_e c^2) \gg 1$ , where  $\epsilon_{ph} \approx kT$  is the photon's energy and  $T$  denotes the temperature of the accretion disk. Radiation power for the Thomson regime is given by:

$$P_T = \frac{\sigma_T \sigma T^4}{4} \frac{\gamma^2}{1 + \frac{\gamma k_B T}{m_e c^2}} \quad (10)$$

and the radiation power in the Klein–Nishina regime writes as (Blumenthal & Gould 1970):

$$P_{KN} \approx \frac{\sigma_T (m_e c k_B T)^2}{16\hbar^3} \left( \ln \frac{4\gamma k_B T}{m_e c^2} - 1.981 \right) \left( \frac{r_s}{r} \right)^2, \quad (11)$$

where  $\sigma_T$  is the Thomson cross section,  $\sigma$  is the Stefan-Boltzman constant,  $k_B$  is Boltzman constant,  $T \approx 8.82 \times 10^4$  is the temperature of the accretion disk ( $T = \left( \frac{GM_{BH}\dot{M}}{8\pi\sigma R_s^3} \right)^{\frac{1}{4}} \left( \frac{R_s}{r} \right)^{\frac{3}{4}} \left( 1 - \sqrt{\frac{R_s}{r}} \right)^{\frac{1}{4}}$  (Carroll & Ostlie 2017) where  $\dot{M} = \pi \left( \frac{GM_{BH}}{a_\infty} \right)^2 \rho_\infty a_\infty$  is accretion rate calculated using Bondi model (Shapiro & Teukolsky 1983)),

#### 3.3. Curvature Radiation

Even if the field lines are almost straight, due to the co-rotation condition, the particles follow the field lines, and therefore, in the laboratory frame of reference, their trajectories might be significantly curved, leading to the mechanism of curvature radiation. The energy loss rate by means of the curvature radiation of the electron is given by (Ruderman & Sutherland 1975)

$$P_{CR} = \frac{2}{3} \frac{e^2 c}{r^2} \gamma^4 \quad (12)$$

The derivation of maximal Lorentz factor considering the IC effect and curvature radiation is not as trivial as it was in the case of co-rotation constrain. While the acceleration power of the electron is more than the electron emission power, the Lorentz factor of the electron is increasing. Therefore, the Lorentz factor will reach its maximum value when acceleration and emission powers balance each other. The corresponding acceleration power is given by:

$$P_{acc} = m_e c^2 \frac{d\gamma}{dt} = 2m_e c \gamma \Omega^2 r \frac{\left(1 - \frac{\Omega^2 r^2}{c^2} - \frac{1}{\gamma^2}\right)^{\frac{1}{2}}}{\left(1 - \frac{\Omega^2 r^2}{c^2}\right)} \quad (13)$$

## 4. Results

Any classical particle is described by its coordinates and velocities. In our case, we can describe an electron by the distance between itself and the LC instead of coordinates, and by  $\gamma$  instead of velocity. From the previous section, we see that all discussed constraints restrict the electron's position and the Lorentz factor. In this section, we will discuss the possible maximal Lorentz factor for an electron accelerated by different types of black holes.

To obtain and clarify the results, we constructed graphs (Figs. 3, 5, 7 and 9) where the so-called allowed and restricted regions are depicted. There are two types of restricted regions: those caused by energy radiation and those caused by the black hole's gravitational and magnetic fields. We call a region restricted and caused by radiation if  $P_{acc} < P_{rad}$ , meaning the

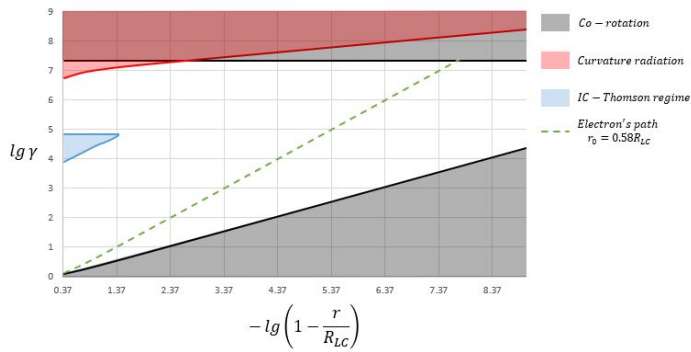


Fig. 3: Map of restricted and allowed regions. Shaded regions represent restrictions with their respective origins. White region represents allowed lorentz factors.  $M_{BH} = 10M_{\odot}$

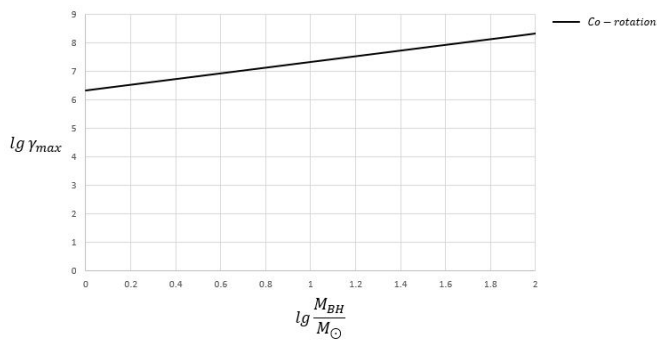


Fig. 4: Possible maximal lorentz factors for Stellar-MBHs

electron loses energy. Conversely, we call a region allowed if  $P_{acc} > P_{rad}$ , meaning the electron gains energy.

Restricted regions due to the IC Thomson scattering are colored in blue, while those due to curvature radiation are colored in red. Restrictions caused by co-rotation constrain is depicted in black and differ from those caused by radiation because in those areas electrons cannot be confined to magnetic field lines, therefore, cannot be accelerated by means of centrifugal acceleration at all. If an electron's energy exceeds a certain threshold or falls below a certain value, it cannot be confined to the magnetic field line, making acceleration with this model impossible. In order to neglect effects of gravitational field, we investigated acceleration process in the region where  $r \gtrsim 0.6R_{LC}$ .

In the next section, we will discuss specific values of  $\gamma_{max}$  for the respective categories of black holes.

#### 4.1. Stellar-Mass black holes (Stellar-MBH)

As we have already mentioned, stellar-mass black holes have masses in the range of  $1 - 100M_{\odot}$ . It appears that only one constraining factor affecting  $\gamma$  in this type of black hole the co-rotation constraint. In Fig. 3, black hole with masses of  $10M_{\odot}$  is presented. From graph, we can see that, in total, all of the constraints can be observed, but only the co-rotation constraint impacts the final Lorentz factor. Thus, regardless of where the electron starts accelerating, the final  $\gamma$  will be the same, approximately  $2 \times 10^7$  in this case.

The possible maximal Lorentz factors for stellar-mass black holes are shown in Fig. 4, with values ranging from  $2 \times 10^6$  to  $2 \times 10^8$ .

#### 4.2. Intermediate-mass black holes (IMBH)

Intermediate-mass black holes (IMBHs) are black holes with masses in the range of  $10^2 - 10^5$  solar masses.

If  $M_{BH} \lesssim 600M_{\odot}$ , the results are qualitatively similar to those for stellar-mass black holes (Stellar-MBHs).

However, if the black hole mass exceeds  $600M_{\odot}$ , curvature radiation becomes significant. For example, in Fig. 5 graph (a), two possible acceleration processes are depicted. The difference between them lies in the starting position of the electron. If an electron begins accelerating closer to the black hole, the final  $\gamma$  will be limited by curvature radiation. But if it starts closer to the LC, then  $\gamma_{max}$  will be constrained by the co-rotation limit, resulting in a range of possible Lorentz factors. For  $M_{BH} = 1000M_{\odot}$ , this range is  $\gamma_{max} \approx 1.4 \times 10^9 - 2 \times 10^9$ .

The second threshold in this mass range occurs at  $M_{BH} \approx 10^4M_{\odot}$ . If  $M_{BH}$  exceeds this threshold, the IC Thomson regime becomes significant. For example, in Fig. 5 graph (b), the results for  $M_{BH} = 10^4M_{\odot}$  show that all constraining factors impact the outcome, although which factor dominates depends on the initial distance from the black hole. In the case of Fig. 5(b), if  $0.58 < r_0 < 0.87$ , then  $\gamma_{max} \approx 1.5 \times 10^4 - 6.7 \times 10^4$ , constrained by the IC Thomson regime. We label this a low-energy result, which is outside our primary focus since numerous other mechanisms can lead to this outcome. When  $r_0 > 0.87$ , the IC Thomson effect no longer constrains the electron's acceleration, allowing it to reach high Lorentz factors above  $10^6$ . At these relativistic factors, the electron is constrained either by the co-rotation limit or curvature radiation, with  $\gamma_{max} \approx 3.8 \times 10^9 - 2 \times 10^{10}$ .

The complete results for IMBHs are shown in Fig. 6, from which we can infer that  $\gamma_{max} \approx 2 \times 10^8 - 2 \times 10^{11}$ .

#### 4.3. Supermassive black holes

In this section, we present results for the largest group of black holes, with masses in the range of  $10^5 - 10^9$  solar masses. For this group, there are only two constraints affecting  $\gamma_{max}$ : co-rotation and curvature radiation. The results for SMBHs with masses  $\lesssim 9 \times 10^5$  are qualitatively the same as for IMBHs with masses over  $10^4M_{\odot}$ .

The threshold in this mass range occurs at  $M_{BH} \approx 10^4M_{\odot}$ . At this point, the radiation power in the IC Thomson regime becomes so strong that an electron in the Thomson regime cannot accelerate at all. Thus, the only way for an electron to accelerate is if it starts in the Klein-Nishina (KN) regime. In this case,  $\gamma \approx 67300$ , which implies that an electron must begin accelerating at  $r_0 \geq (1 - 10^{-10})R_{LC}$ , as shown in Fig. 7. In Fig. 8, we can see that the possible maximal Lorentz factors for SMBHs range from  $2.5 \times 10^{10}$  to  $2 \times 10^{15}$ .

#### 4.4. Ultramassive black holes

As we have already mentioned, another category of black holes is sometimes considered for those with masses over  $10^9M_{\odot}$ , such as the one at the center of Abell 1201. In this section, we present results specifically for that black hole. The mass of these black holes is immense, resulting in a low angular velocity. Consequently, the acceleration power is much smaller than the radiation power in the inverse Compton Thomson regime. Thus, the only feasible way for an electron to accelerate is to do so very close to the LC, the same as for SMBHs and IMBHs with masses exceeding  $9 \times 10^5M_{\odot}$ , as described in the respective subsections. From Fig. 9, it can be inferred that the lower bound for  $\gamma_{max}$  is set by curvature radiation, approximately equaling  $1.1 \times 10^{13}$ . Con-



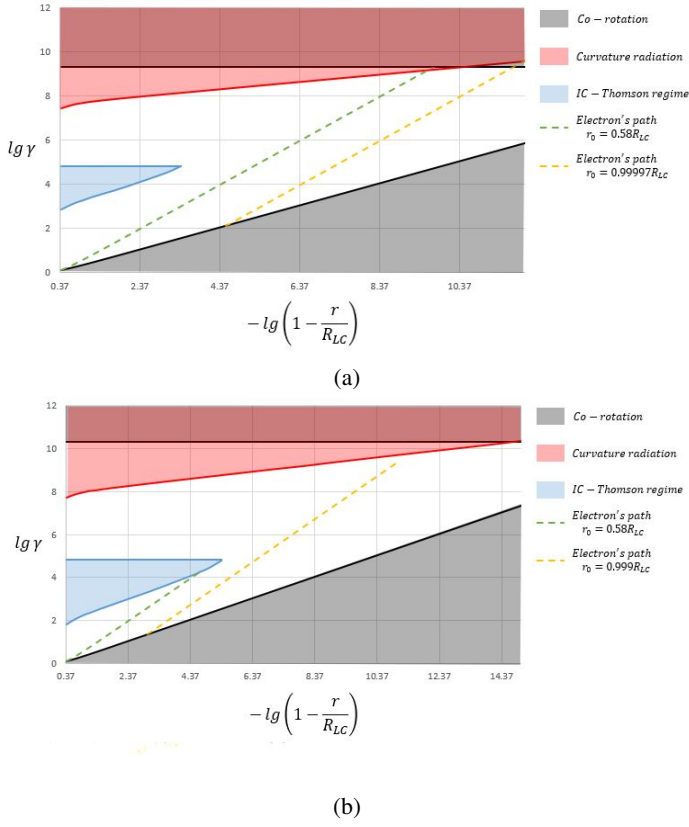


Fig. 5: Map of restricted and allowed regions. Shaded regions represent restrictions with their respective origins. White region represents allowed Lorentz factors (a)  $M_{BH} = 1000M_{\odot}$  (b)  $M_{BH} = 10^4M_{\odot}$

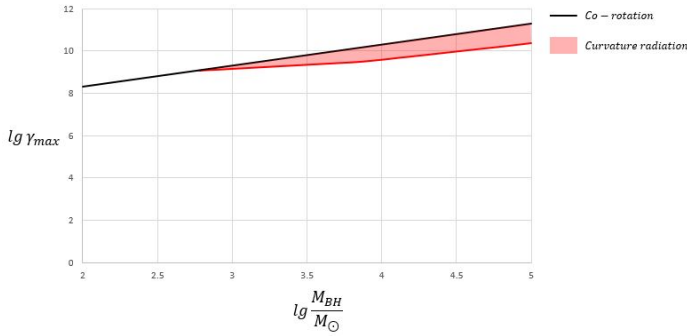


Fig. 6: Possible maximal Lorentz factors for IMBHs

versely, the upper bound for  $\gamma_{max}$  is defined by the co-rotation constraint and is  $6.6 \times 10^{16}$ . Therefore,  $\gamma_{max}$  is in the range of  $1.1 \times 10^{13}$  to  $6.6 \times 10^{16}$

## 5. Conclusions

In the present work, we examine centrifugal acceleration as an efficient mechanism for electrons to achieve high energies. We consider electrons confined to a straight magnetic field line, with their acceleration limited by several constraining factors: the inverse Compton effect, curvature radiation, and the breakdown of particle-to-field-line confinement. Our study focuses on investigating how the maximal energy and the main constraining factor

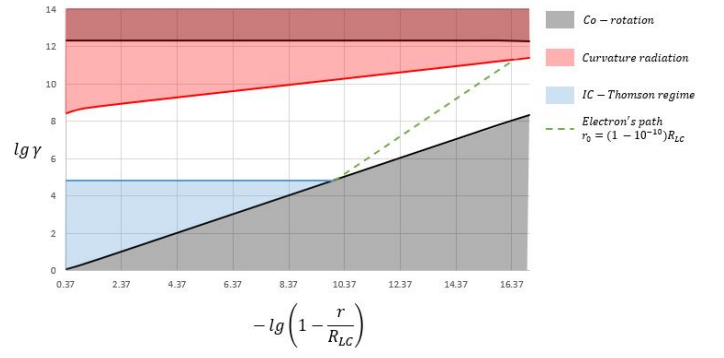


Fig. 7: Map of restricted and allowed regions. Shaded regions represent restrictions with their respective origins. White region represents allowed Lorentz factors.  $M_{BH} = 10^6$

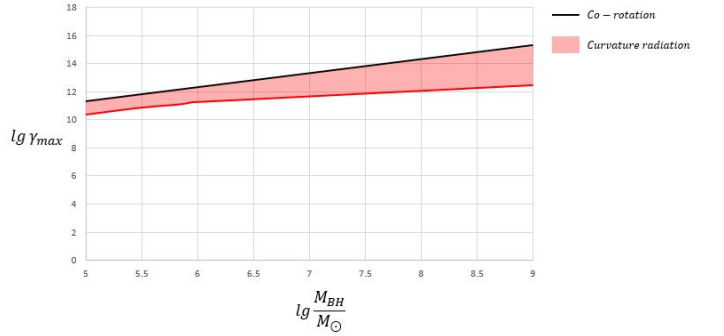


Fig. 8: Possible maximal Lorentz factors for SMBHs

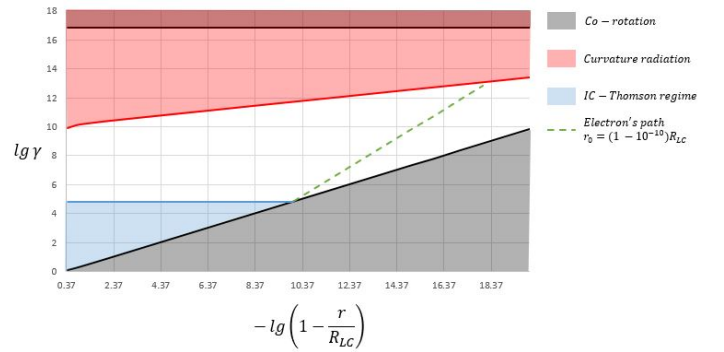


Fig. 9: Map of restricted and allowed zones for electron in the magnetosphere of the ultramassive black hole in the center of Abell 1201

depend on the mass of a black hole, with a particular emphasis on intermediate-mass black holes (IMBHs) and ultra-massive black holes (UMBHs), as these have not been extensively investigated before. Additionally, we investigate how maximal relativistic factors change due to the initial location of the particle.

It appears that, even for a given black hole, the maximal electron energy depends on where the particle starts the acceleration process (whether closer to or further from the black hole). Therefore, the maximal energy is a range rather than a distinct value. For stellar-mass black holes (Stellar-MBHs) the only constraining factor is the co-rotation constraint, and regardless of where the particle begins acceleration, the maximal energy remains the same. For stellar-MBHs, the Lorentz factor is within the range of  $2 \times 10^6$  to  $2 \times 10^8$ .

The case of IMBHs is particularly intriguing as it presents two critical threshold points at  $600M_{\odot}$  and  $10^4M_{\odot}$ . If  $M_{BH}$  exceeds critical value of  $600M_{BH}$ , final relativistic factor can be affected by curvature radiation, depending on where the electron starts acceleration process. If  $M_{BH}$  exceeds  $10^4M_{\odot}$ , particles accelerated closer to the black hole become strongly affected by the inverse Compton effect in the Thomson regime, requiring particles to start accelerating closer to the LC to achieve high energies since ones that start closer to BH are bound by IC - Thomson emission. More concisely, their start position has to be  $r_0 \geq (1 - 10^{-10})R_{LC}$ . For IMBHs, the range of maximal Lorentz factors is approximately  $2 \times 10^8$  to  $2 \times 10^{11}$ .

SMBHs with masses less than  $9 \times 10^5 M_{\odot}$ , accelerate particles qualitatively the same as IMBHs, but when the threshold value of  $9 \times 10^5 M_{\odot}$  is reached, IC - Thomson radiation becomes so strong that electrons need to have initial Lorentz factors of the order of  $10^4$ , therefore need to be confined very close to the LC, in order to start acceleration process. For SMBHs, the range of maximal electron Lorentz factors spans from  $2.45 \times 10^{10}$  to  $2 \times 10^{15}$ . As an example of a UMBH, we investigate the ultra-massive black hole at the center of Abell 1201, where the range of Lorentz factors is approximately  $1.1 \times 10^{13}$  to  $6.6 \times 10^{16}$ .

## 6. Acknowledgments

The research of N.N. was supported by the Knowledge Foundation of the Free University of Tbilisi and the work of Z.O. was supported by Shota Rustaveli National Science Foundation of Georgia (SRNSFG). Grant: FR-23-18821

## References

- Bell, A. R. 1978a, MNRAS, 182, 147  
 Bell, A. R. 1978b, MNRAS, 182, 443  
 Blandford, R. D. & Znajek, R. L. 1977, MNRAS, 179, 433  
 Blumenthal, G. R. & Gould, R. J. 1970, Rev. Mod. Phys., 42, 237  
 Bondi, H. 1952, MNRAS, 112, 195  
 Carroll, B. W. & Ostlie, D. A. 2017, An Introduction to Modern Astrophysics, 2nd edn. (Cambridge University Press)  
 Catanese, M. & Weekes, T. C. 1999, PASP, 111, 1193  
 Fermi, E. 1949, Phys. Rev., 75, 1169  
 Goldreich, P. & Julian, W. H. 1969, Astrophysical Journal, 157, 869  
 Kızıltan, B., Baumgardt, H., & Loeb, A. 2017, Nat, 542, 203  
 Nightingale, J. W., Smith, R. J., He, Q., et al. 2023, MNRAS, 521, 3298  
 Osmanov, Z. 2021, Galaxies, 9, 6  
 Osmanov, Z. & Rieger, F. M. 2009, A&A, 502, 15  
 Osmanov, Z. & Rieger, F. M. 2016, MNRAS, 464, 1347  
 Osmanov, Z., Rogava, A., & Bodo, G. 2007, A&A, 470, 395  
 Rieger, F. M. 2011, International Journal of Modern Physics D, 20, 1547  
 Rieger, F. M. & Mannheim, K. 2000, A&A, 353, 473  
 Rogava, A., Dalakishvili, G., & Osmanov, Z. 2003, Gen. Rel. and Grav., 35, 1133  
 Ruderman, M. A. & Sutherland, P. G. 1975, ApJ, 196, 51  
 Shapiro, S. L. & Teukolsky, S. A. 1983, Black holes, white dwarfs and neutron stars. The physics of compact objects (John Wiley & Sons, Ltd)